Optimal, Nonlinear, and Distributed Designs of Droop Controls for DC Microgrids

Ali Maknouninejad, *Member, IEEE*, Zhihua Qu, *Fellow, IEEE*, Frank L. Lewis, *Fellow, IEEE*, and Ali Davoudi, *Member, IEEE*

Abstract—In this paper, the problem of optimal voltage and power regulation is formulated for distributed generators (DGs) in DC microgrids. It is shown that the resulting control is optimal but would require the full information of the microgrid. Relaxation of information requirement reduces the optimal control into several controls including the conventional droop control. The general setting of a DC microgrid equipped with local sensing/communication network calls for the design and implementation of a cooperative droop control that uses the available local information and coordinates voltage control in a distributed manner. The proposed cooperative droop control is shown to include other controls as special cases, its performance is superior to the conventional droop control, and it is robust with respect to uncertain changes in both distribution network and sensing/communication network. These features make the proposed control an effective scheme for operating a DC microgrid with intermittent and distributed generation.

Index Terms—Conventional droop control, cooperative droop control, DC microgrid, distributed generation, distribution network, smart grid.

I. INTRODUCTION

THE electricity demand, combined with physical, economical and environmental constraints of conventional energy sources such as fossil and nuclear energy, is putting more emphasis on finding and utilizing alternative energy sources. Of special interest are renewable energy sources such as solar and wind energy generation. This has lead to the emergence of distributed generators (DGs), self-organizing microgrids, and smart grid. DGs may be heterogeneous as PV systems, wind turbines, fuel cells, and diesel generators. DG locations must be economically and physically feasible. To better harness alternative energy or to serve critical loads, DGs are installed at the most economical and physically-feasible locations, and they are often dispersed widely across the distribution network. To properly control and manage these DGs, it is natural to organize DGs in a given geographical area into a self-organizing microgrid
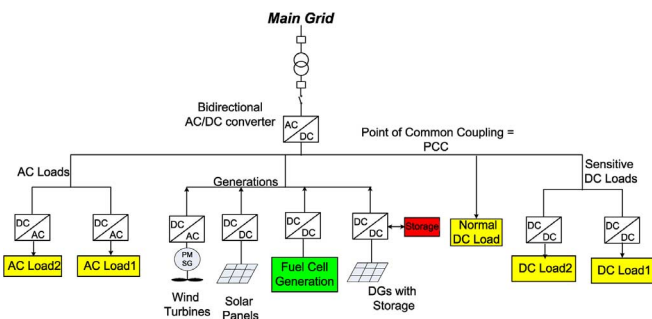
Fig. 1. A general block diagram of a typical DC microgrid.

which is connected to the main grid through point of common coupling (PCC).

In current distribution networks, microgrids are in the AC form. A DC microgrid may coexist with the rest of the AC grid, power generation plants, and transmission networks. Many of DGs are in a DC form and, in order to have an AC system, DGs can use a DC/AC inverter stage to convert their DC current/voltage into a grid quality AC current/voltage, but this extra stage increases cost and reduces efficiency. Therefore, there is resurgence of interests in DC microgrids, while the concept of DC microgrids were discussed in [1].

A typical structure of a DC microgrid [1] is shown in the Fig. 1. At the PCC, the microgrid is connected to the main grid through one bidirectional AC/DC converter (rather than several DC/AC inverters). In the microgrid, renewable energy sources and other DGs are connected to DC buses through DC/DC converters. Regular DC loads may be connected directly to any of DC buses, and critical DC loads that require an exact voltage regulation may utilize DC/DC converters at their connection points. Storage devices may or may not be affiliated with DGs. Similar to an AC microgrid, a hierarchical and multi level control may be applied to control the DGs power generation and storages, to optimize the interests of both the microgrid/main-grid and individual devices, while securing the system stability [2]. However, as will be discussed in the subsequent discussions, cooperative droop control as an improved droop control may be applied at the level of DGs and storage units to guarantee the system stability and proper utilization of available resources in the microgrid, including DGs and storage.

Potential advantages of a DC microgrid over the AC counterpart can be summarized as follows:

1) The majority of renewable energy sources (e.g., photovoltaic) and storage systems (e.g., batteries) are natively DC. Emerging new loads are either DC loads (e.g., data centers) or AC loads that are driven by DC sources (e.g., inverter-fed AC machines). It has been shown in [3], [4] that

DC microgrids are about two orders-of-magnitudes more available than their ac counterparts.

2) DC microgrids have simpler models and controls (i.e., no phase angle or frequency or reactive power), while synchronization, reactive power flow and harmonics have to be considered for ac systems.

3) DC microgrids would significantly improve system reliability, efficiency, and economy by eliminating the DC/AC/DC conversion stages [5], [6]. Since reactance has little effect, a cable could carry more DC power than AC power [1], [7].

Some of the challenges associated with DC distribution systems have been investigated in [1]. In particular, the interaction between different power converters and neutral voltage shifts are discussed. A technique of connecting the microgrid to and disconnecting the microgrid from the main power system is studied by [8]. An energy management system (EMS) is proposed in [9] to incorporate into a DC distribution system the charge and discharge of electric vehicles.

There is an abundance of research and literature covering AC microgrids and DGs management [10]–[16], but an investigation into the microgrid/grid level control of DGs in a DC microgrid remains open to investigation. One exception is [17] in which applications of the conventional droop control to both DC and AC microgrids are investigated. This paper aims at developing systematic designs and analysis for controlling DC microgrids.

In this paper, the problem of voltage and power regulation by DGs in a DC microgrid is formulated as an optimal control problem, and the resulting optimal control is used as the seed controller to investigate its variations in terms of information needed. By further advancing the application of cooperative control from AC network [2], [18]–[20] to DC microgrids, a distributed droop control (called cooperative droop) is proposed. The main objective of cooperative droop control is to utilize the available information (from low-bandwidth local communication links) and to improve the overall voltage profile by coordinating the neighboring control actions.

II. DC MICROGRID MODEL FORMULATION

Consider a DC microgrid which consists of n nodes and whose circuit network has the following admittance matrix

$$Y = [Y_{ij}] \in \Re^{n_p \times n_p}, \ Y_{ij} = \begin{cases} y_i + \sum_{l \neq i} y_{il} & \text{if } i = j \\ -y_{ij} & \text{if } i \neq j \end{cases} \quad (1)$$

where $y_{ij} = y_{ji}$ is the line admittance between nodes i and j, and y_i is the admittance between node i and the ground, if there is any. Topology of the microgrid can be represented by a physical-connectivity graph $(\mathcal{V}_p, \mathcal{E}_p)$, where $\mathcal{V}_p$ denotes the set of $(n_p + 1)$ nodes (with the $(n_p + 1)$th node being the ground) and $\mathcal{E}_p$ denotes the set of undirected edges (for which $y_{ij} \neq 0$ or $y_i \neq 0$).

The microgrid contains m DGs (whether they are PV, wind, biomass, or their combinations) and, if it is grid-tied, the power from the grid (of node 0) is injected into node 1. These DGs may have different dynamics, and the use of power electronic devices will be a common practice for connecting DGs to the rest of the system in the future smart grids. Such power electronic converters have a fast transient response, in terms of few mil-

liseconds or faster, and upon applying the feedback linearization method, their dynamics are assumed to be

$$\tau_i \dot{P}_{g_i} = -P_{g_i} + u_i, \quad i \in \mathcal{V}_g, \quad (2)$$

where $\tau_i > 0$ is the time constant (whose value is typically small), and $\mathcal{V}_g \subset \mathcal{V}_p$ is the index set of those nodes where there are DGs installed. Variables u_i and P_{g_i} are the power command and the actual power output of the ith DG, respectively. Accordingly, the power flow equations of the DC microgrid are given by

$$P_{g_i} - P_{l_i} = V_i \sum_{j \in \mathcal{V}_p} y_{ij}(V_i - V_j), \quad (3)$$

where $P_{g_i} = 0$ if $i \notin \mathcal{V}_g$, V_i is the voltage at node i, and P_{l_i} represents the load at node i.

All of the electrical and control variables in (2) and (3) are assumed to be of per-unit values. The objective of the proposed control designs is threefold: i) Ensure exponential stability under constraints of (3); ii) achieve the goal of $V_i \in (0.95, 1.05)$ and minimize the loss as much as possible; iii) design the best control with respect to available information. Three information patterns will be investigated: weakly global information of V_i, decentralized information of V_i, and distributed information of V_i. The distributed information structure is represented by an intermittent sensing/communication digraph $(\mathcal{V}_s, \mathcal{E}_s(t))$, where $\mathcal{V}_s$ denotes the set of n_s nodes (or $(n_s + 1)$ nodes including node 0 if grid tied) and $\mathcal{E}_s(t)$ denotes the set of directed edges. Alternatively, the local information flow can be characterized by the binary sensing/communication matrix

$$S(t) = [s_{ij}(t)] \in \Re^{n_s \times n_s}, \quad (4)$$

where $s_{ii}(t) \equiv 1$, $s_{ij}(t) = 1$ if $\{j \to i\} \in \mathcal{E}_s(t)$ (i.e., V_j is available to node i at the time t), and $s_{ij}(t) = 0$ if otherwise. At time t, the neighboring set $\mathcal{N}_i(t)$ of node i consists of those nodes from which communication is received (i.e., $\mathcal{N}_i(t) = \{j : s_{ij}(t) = 1\}$).

III. BASIC DESIGNS OF OPTIMAL CONTROL AND DROOP CONTROL

In this section, an optimal design framework is presented to derive a nonlinear optimal control. It is shown that this seed control design can reduce to a linear global-information voltage-feedback control, a decentralized droop control, and an adaptive control. The discussions provide the motivations for designing a distributed droop control in the subsequent section.

A. An Optimal Design

The following theorem provides an optimal control as the seed controller in the subsequent analysis, and its proof is included in Appendix A.

Theorem 1: Consider the DC microgrid consisting of DGs in (2) and under the control law

$$u_i = -\frac{k_i^2}{\sqrt{1 + k_i^2}} \left(V_i - V_i^*\right) \left[\sum_{j \in \mathcal{V}_p} y_{ij} \left(V_i - V_j + V_i^*\right)\right]$$

$$+ \frac{k_i^2}{\sqrt{1 + k_i^2}} \sum_{j \in \mathcal{V}_p} y_{ij} \left(V_j - V_j^*\right) + \frac{k_i^2}{1 + k_i^2 + \sqrt{1 + k_i^2}} P_{g_i}, \quad (5)$$
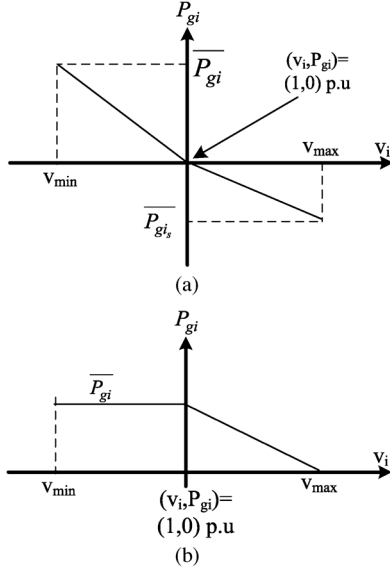
Fig. 2. Droop curves for DGs with and without storage. (a) Droop curve for DGs with storage; (b) droop curve for DGs without storage.

where $P_{g_i}^*$ and V_i^* satisfy power flow (3). Then, control (5) is optimal with respect to performance index

$$J = \sum_{i \in \mathcal{V}_p} \left[\beta_i \tau_i \left[P_{g_i}(T) - P_{g_i}^* \right]^2 + \int_{t_0}^{T} \left[k_i^2 \left(P_{g_i} - P_{g_i}^* \right)^2 + u_i^2 \right] dt \right],$$ (6)

where $T > 0$ is given, and $\beta_i = k_i^2 / (\sqrt{1 + k_i^2} + 1)$. Furthermore, the control ensures that P_{g_i} converges globally and exponentially to its steady state of $P_{g_i}^* / (1 + k_i^{-2})$.

Should control (5) be implemented, desired values $P_{g_i}^*$ and V_i^* need to be chosen. Its implementation also requires y_{ij}, that is, all the information about the DC microgrid. In what follows, several choices and simplifications are investigated.

B. Uniform Terminal Voltages Under Unconstrained DGs

If DGs have sufficient capacity/storage capability, $P_{g_i}^*$ could be chosen such that $V_i^* \approx 1$ for all $i \in \mathcal{V}_g$. In this case, control (5) becomes

$$u_i = -\frac{k_i^2}{\sqrt{1 + k_i^2}}(V_i - 1) \left[\sum_{j \in \mathcal{V}_p} y_{ij}(V_i - V_j + 1) \right]$$

$$+ \frac{k_i^2}{\sqrt{1 + k_i^2}} \sum_{j \in \mathcal{V}_p} y_{ij} \left(V_j - V_j^* \right) + \frac{k_i^2}{1 + k_i^2 + \sqrt{1 + k_i^2}} P_{g_i}, \quad (7)$$

which remains to be nonlinear. The linearized version of control (7) around $\{V_i^* \approx 1, i \in \mathcal{V}_g\}$ and $\{V_j^*, j \notin \mathcal{V}_g\}$ is

$$u_i = -\frac{k_i^2}{\sqrt{1 + k_i^2}}(V_i - 1) \left[\sum_{j \in \mathcal{V}_p} y_{ij} \left(2 - V_j^* \right) \right]$$

$$+ \frac{k_i^2}{\sqrt{1 + k_i^2}} \sum_{j \in \mathcal{V}_p} y_{ij} \left(V_j - V_j^* \right) + \frac{k_i^2}{1 + k_i^2 + \sqrt{1 + k_i^2}} P_{g_i}. \quad (8)$$

Applying the approximation of $V_j^* \approx 1$ to (8) yields

$$u_i = -k_{ii}'(V_i - 1) + \sum_{j \in \mathcal{V}_p} k_{ij}'(V_j - 1) + (1 - \varepsilon_i)P_{g_i} \quad (9)$$

in which

$$k_{ii}' = \frac{k_i^2}{\sqrt{1 + k_i^2}} \sum_{j \in \mathcal{V}_p} y_{ij}, \; k_{ij}' = \frac{k_i^2}{\sqrt{1 + k_i^2}} y_{ij},$$

$$\varepsilon_i = \frac{1 + \sqrt{1 + k_i^2}}{1 + k_i^2 + \sqrt{1 + k_i^2}},$$

and the sum of all the coefficients associated with $(V_i - 1)$ and $(V_j - 1)$ is zero (that is, $\sum_{j \in \mathcal{V}_p} k_{ij}' = k_{ii}'$).

It follows from the preceding discussions that control (9) is near-optimal. In addition, control (9) does not require any information about the loads but weakly global information of line admittance and voltages (that is, every node receives the information of the voltages from all physically-connected nodes).

C. Decentralized Droop Control

In the case that the weakly global information of line admittance and voltages is not available, one can choose to ignore the terms $(V_j - 1)$ in (9). By doing so, one obtain the following droop control:

$$u_i = -k_{ii}(V_i - 1) + (1 - \varepsilon_i)P_{g_i}, \quad (10)$$

where k_{ii} is a positively-valued lumped gain chosen by the designer (so that line admittances are no longer needed), and $\varepsilon_i \in (0, 1)$.

Fig. 2 shows the related droop characteristic for individual DGs, with or without storage. As it is seen, the droop gain for the voltages above and below the unity are different. The reason is that when the voltage is below the unity, DGs generate power to increase the voltage and the generation limit is set by their available active power, $\overline{P}_{g_i}$. If DGs do not have storage available, they need to generate all their available active power at this voltage range; otherwise they may follow the linear relation curve as in Fig. 2(a) and charge their storages when they generate less power than their available one, as voltage rises to unity.

On the other hand, when the voltage is below the unity, mainly due to the excessive generated active power, if DGs have storage, they absorb active power from the grid. The limit for the active power absorbtion is set by the DGs storage devices capacity, $\overline{P}_{g_{i_s}}$. DGs without available storage, linearly reduce their generation down to zero at V_{max} [16].

The characteristic curves in the Fig. 2 goes well along with the concept of the fair utilization ratio, initially introduced in [2], [19] for AC systems.

Control (10) is decentralized and hence the simplest to be implemented, but its transient and steady-state performance is often inferior. In a smart DC grid, distributed information are available and hence should be used to synthesize distributed (cooperative) controls, which is the subject of the subsequent section.

D. Adaptive Control

For sufficiently large values of k_i and for $\epsilon_i = 0$, control (10) becomes

$$u_i = -k_{ii}(V_i - 1) + P_{g_i}, \quad (11)$$

under which DG dynamics (2) becomes $\tau_i \dot{P}_{g_i} = -k_{ii}(V_i - 1)$, which acts as a pure integrator to ensure $V_i^* = 1$ independent

of microgrid's load condition. Using the adaptive control terminology [21], control (11) is an adaptive control, and droop control (10) is an adaptive control law with a small leakage. Similar argument holds for near-optimal control (9) and nonlinear optimal control (5).

IV. COOPERATIVE DROOP CONTROL OF DC MICROGRID

The proposed cooperative droop control (based on distributed information) is

$$u_i = d_{ii}(t)(V_i - 1) + \sum_{j \in \mathcal{N}_i} d_{ij}(t)(V_j - 1) + (1 - \epsilon_i)P_{g_i}, \quad (12)$$

where α_{ij} are positive gains, $\varepsilon_i \in (0, 1)$ is a leakage constant (of small value), and

$$d_{ij}(t) = \begin{cases} \frac{\alpha_{ij}s_{ij}(t)}{\sum_{l=1}^{n_s} \alpha_{il}s_{il}(t)} & \text{if } j \neq i \\ -\sum_{j \in \mathcal{N}_i} d_{ij}(t) & \text{if } j = i. \end{cases} \quad (13)$$

By the above definition, $D = [d_{ij}]$ is a Metzler matrix (i.e., all its off-diagonal elements are non-negative) and it has zero row sums. That is, $-D$ is the Laplacian of the information network corresponding to distributed control (12).

Based on the available communication links and the selection of α_{ij} gains, the following control scenarios are viable:

1) If $s_{ij} = 0$ for all $i \neq j$ (i.e., not sharing information at all), cooperative droop control (12) no longer has any coordination and reduces to the conventional droop control (10).

2) If $s_{ij} = 1$ for all the physically connected nodes, cooperative control (12) with $d_{ij} = k'_{ij}$ becomes near-optimal control (9); and, should weakly global information be available, a nonlinear version of cooperative droop control (12) would become the nonlinear optimal control (7).

3) By setting $\varepsilon_i = 0$, the cooperative droop control becomes the following cooperative adaptive control:

$$u_i = -(V_i - 1)\sum_{j \in \mathcal{N}_i} d_{ij}(t) + \sum_{j \in \mathcal{N}_i} d_{ij}(t)(V_j - 1) + P_{g_i}. \quad (14)$$

Cooperative droop control (12) has the unique feature of accommodating intermittent and local communication networks, and its stability analysis calls for the following lemma whose proof is included as Appendix B.

Lemma 1: Suppose that power flow (3) has steady-state solution pair $P_{g_i}^*$ and V_i^*. Then, around the steady state,

$$P_g - P_g^* = H_{gg}\left(V_g - V_g^*\right), \quad (15)$$

where $P_g = \text{vec}\{P_{g_i}\}$ for $i \in \mathcal{V}_g$, $V_g = \text{vec}\{V_i\}$ for $i \in \mathcal{V}_g$, and matrix H_{gg}^{-1} is a positive matrix, the relative values of off-diagonal entries in H_{gg}^{-1} are monotonely increasing functions of the physical distances among the DGs.

Stability and convergence of cooperative droop control (12) is ensured by the following theorem, and the stability proof can be found in Appendix C. The theorem also provides formal stability analysis for conventional droop control (10).

Theorem 2: Consider the DC microgrid consisting of DGs in (2) and with power flow (3). Then, cooperative droop control (12) ensures that, for all reasonable ranges of node voltages, their steady states converge to values close to 1 if eigenvalues of product $A \triangleq DH_{gg}^{-1}$ are Lyapunov stable (equivalently, there is a positive-definite matrix M such that $\{MA + A^{TM}\}$ is negative semi-definite). Furthermore, as the sensing/communication network has more connectivity, the corresponding state-steady node voltages become closer to 1 than those under the conventional droop control.

It is well known that the eigenvalue test and Lyapunov function matrix M in theorem 2 are equivalent. It is also known (see theorem 4.31 in [18]) that, if matrix A is a Metzler matrix as matrix D, simple conditions are available to verify the existence of Lyapunov matrix M and matrix M can be simply diagonal. Furthermore, if A is Metzler and symmetric and has zero row sums, $M = I$. Unfortunately, A being Metzler may not hold for all DC microgrids.

As an example, consider the microgrid system shown in the Fig. 3. The microgrid has eight DGs, and its physical topology and line resistances yield the admittance matrix at the bottom of the page. Suppose that the sensing/communication network among the DGs is represented by

$$S = \begin{bmatrix} 1 & 0 & 0 & 1 & 0 & 0 & 1 & 0 \\ 0 & 1 & 1 & 0 & 0 & 0 & 1 & 1 \\ 1 & 1 & 1 & 1 & 0 & 0 & 0 & 1 \\ 1 & 0 & 0 & 1 & 1 & 1 & 0 & 0 \\ 0 & 0 & 0 & 1 & 1 & 0 & 0 & 0 \\ 0 & 0 & 0 & 1 & 0 & 1 & 0 & 1 \\ 0 & 1 & 0 & 1 & 1 & 0 & 1 & 1 \\ 0 & 0 & 0 & 1 & 1 & 0 & 1 & 1 \end{bmatrix}. \quad (16)$$

Then, the simplest choices of $\alpha_{ij} = 1$ for all i and j renders matrix D as the first equation at the bottom of the next page.

It is straightforward to verify that $A = DH_{gg}^{-1}$ is given by the second equation at the bottom of the next page, which has the desired stability property but is not a Metzler matrix.

$$H_{gg} = \begin{bmatrix} 20.24 & 0 & 0 & 0 & 0 & 0 & 0 & -20.24 \\ 0 & 95.76 & -72.11 & 0 & 0 & 0 & 0 & -24.91 \\ 0 & -140.40 & 143.86 & 0 & 0 & 0 & 0 & 0 \\ 0 & 0 & 0 & 9.49 & 0 & 0 & 0 & -9.51 \\ 0 & 0 & 0 & 0 & 858.04 & -763.70 & 0 & -94.34 \\ 0 & 0 & 0 & 0 & -476.19 & 476.19 & 0 & 0 \\ 0 & 0 & 0 & 0 & 0 & 0 & 76.92 & -76.92 \\ -19.55 & -38.87 & 0 & -10.17 & -42.37 & 0 & -76.92 & 526.45 \end{bmatrix}.$$
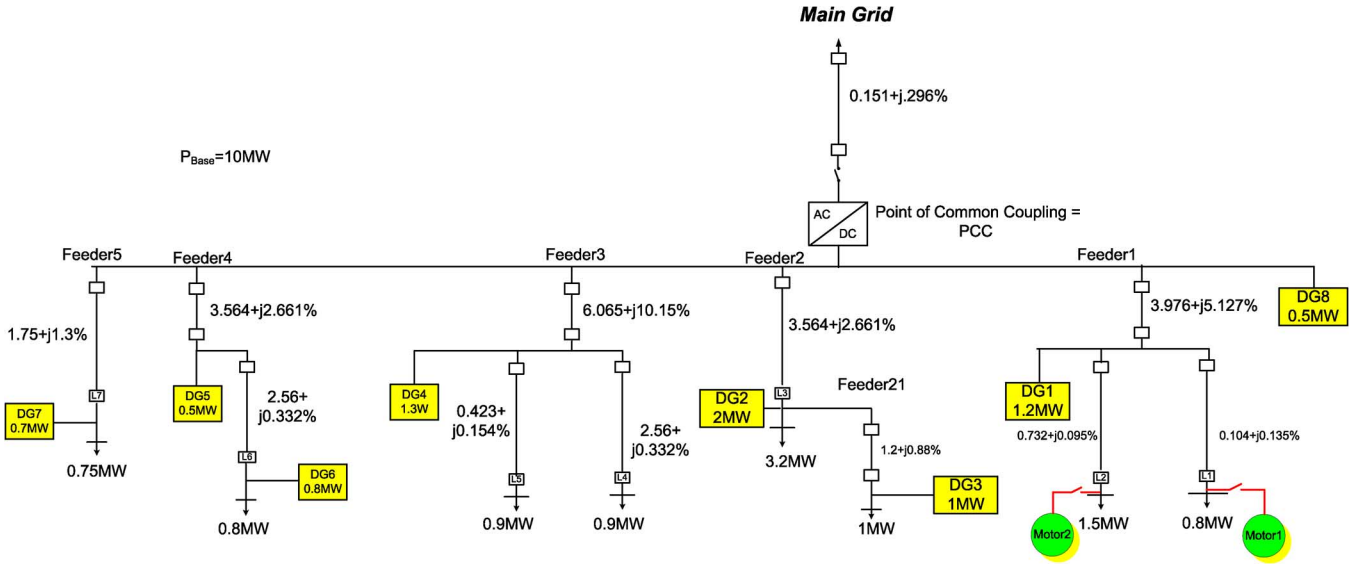
Fig. 3. A case study of DC microgrid.

It is important to note that design parameters α_{ij} (which determine matrix D) can be chosen without exact knowledge of microgrid's distribution network. Given an approximate topology of microgrid's distribution network, a rough estimate $\hat{H}_{gg}$ of H_{gg} can be obtained for the purpose of inspection. Although H_{gg} and $\hat{H}_{gg}$ would be different, the same control design is applicable. As an illustration, reconsider the microgrid system shown in the Fig. 3. Should there be a 10% increase of the impedance at feeder21 and a 10% decrease of the impedances at feeder 4, matrix H_{gg} becomes the first equation at the bottom of the next page. Then, for the same choices of $\alpha_{ij} = 1$ and under the same sensing/communication topology S, the resulting matrix $A = DH_{gg}^{-1}$ is given by the second equation at the bottom of the next page, which has the desired

stability property as before. It is also worth noting that control parameters α_{ij} are chosen independently of specific connectivity matrix S. These robustness properties (with respect to the changes of both physical network and sensing/communication network) make the proposed cooperative droop control uniquely effective for microgrids with intermittent operation of DGs. Further analysis of robustness can be rigorously done by integrating robust control theory [22] into cooperative control design, but this is beyond the scope of this paper.

V. CASE STUDIES AND PERFORMANCE COMPARISONS

In this section, two case studies are carried out for the microgrid system shown in the Fig. 3. Topologically, the DC microgrid is connected to the main grid at the point of common

$$
D = \begin{bmatrix}
-0.67 & 0 & 0 & 0.33 & 0 & 0 & 0.33 & 0 \\
0 & -0.75 & 0.25 & 0 & 0 & 0 & 0.25 & 0.25 \\
0.20 & 0.20 & -0.80 & 0.20 & 0 & 0 & 0 & 0.20 \\
0.25 & 0 & 0 & -0.75 & 0.25 & 0.25 & 0 & 0 \\
0 & 0 & 0 & 0.50 & -0.50 & 0 & 0 & 0 \\
0 & 0 & 0 & 0.33 & 0 & -0.67 & 0 & 0.33 \\
0 & 0.20 & 0 & 0.20 & 0.20 & 0 & -0.80 & 0.20 \\
0 & 0 & 0 & 0.25 & 0.25 & 0 & 0.25 & -0.75
\end{bmatrix}.
$$

$$
A = \begin{bmatrix}
-0.0329 & 0 & 0 & 0.0351 & 0 & 0 & 0.0043 & 0 \\
0 & -0.0199 & -0.0082 & 0 & 0 & 0 & 0.0033 & 0 \\
0.01 & -0.0227 & -0.0170 & 0.0212 & 0 & 0.0001 & 0.0001 & 0.0001 \\
0.0123 & 0 & 0 & -0.0791 & 0.0053 & 0.009 & 0 & 0 \\
0 & 0 & 0 & 0.0527 & -0.0053 & -0.0085 & 0 & 0 \\
0 & 0 & 0 & 0.0351 & -0.0071 & -0.0127 & 0 & 0 \\
0 & 0.0079 & 0.0039 & 0.0211 & 0.0021 & 0.0034 & -0.0104 & 0 \\
0 & 0 & 0 & 0.0264 & 0.0027 & 0.0043 & 0.0030 & 0
\end{bmatrix},
$$

coupling and through the AC/DC converter at the top. The converter is to maintain a grid-tied operation and meet the demand of all the loads by converting the grid AC voltage into a DC one, suitable for the DC microgrid operation. There are a total of eight DGs distributed across the microgrid, and they have a total of 15.5 MVA generation capacity. In particular, it is assumed that DGs 2, 3 and 4 are wind farms and that DGs 1, 5, 6, 7, and 8 are solar farms.

Two operational scenarios are simulated to compare the performance of conventional droop control (10) and the proposed cooperative droop control (12). For the conventional droop, its droop gains are chosen based on the Fig. 2; specifically in (10) together with (2), the gain is chosen as $k_{ii} = \overline{P}_{gi}/0.05 = 20\overline{P}_{gi}$ if $V_i < 1$ p.u. or $k_{ii} = \overline{P}_{gi_s}/0.05 = 20\overline{P}_{gi_s}$ if $V_i > 1$ p.u., where $\overline{P}_{gi}$ and $\overline{P}_{gi_s}$ are the rated capacity of generation and storage, respectively. In the first scenario, DGs are operating at 50% of their rated capacity. In the second scenario, DGs' available power are determined by their profiles in the Fig. 7. For each DG, per unit is based on its own capacity and not the microgrid power base; e.g., in Fig. 7, DG1 has 1 p.u. power available or 1.2 MW power available, based on its rated capacity shown in Fig. 3. For cooperative adaptive droop control (14), design gains are chosen as $\alpha_{ij} = 1$ for all $i, j = 1, \cdots, 8$. It is assumed that the sensing/communication topology is given by (16).

As the first operational scenario, the DGs are connected to the system at $t = 0.4$ s. Afterwards, a 300 KW DC motor is connected to the feeder1 at $t = 1$ s, which causes a transient voltage dip in the microgrid. The two control options, either conventional droop control (10) and the proposed cooperative droop control (12), are implemented at the DGs to regulate their node voltages. Figs. 4 and 5 show the voltages at DG3 and DG6, similar changes are observed at all other DG nodes, and Fig. 6 provides the norm of the voltage deviations from unity at these DG nodes. In these three figures, the conventional droop control
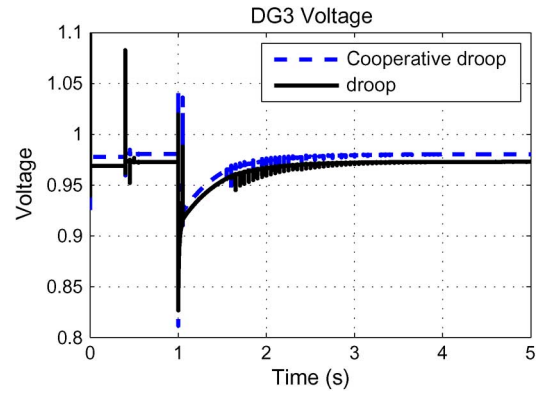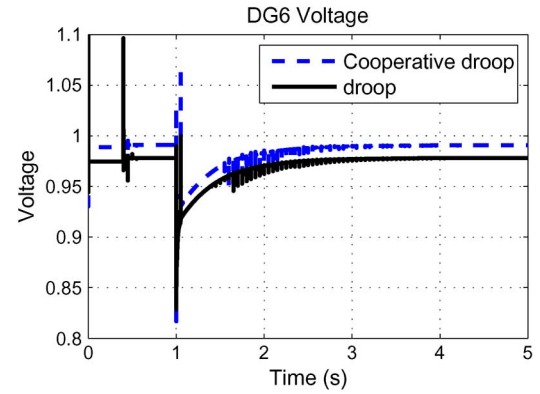

Fig. 4. Voltage of DG3.

Fig. 5. Voltage of DG6.

and the proposed cooperative droop control are compared, and it is apparent that the cooperative droop control has a superior performance.

$$H_{gg} = \begin{bmatrix} 19.46 & 0 & 0 & 0 & 0 & 0 & 0 & -19.46 \\ 0 & 151.35 & -113.64 & 0 & 0 & 0 & 0 & -39.25 \\ 0 & -110.84 & 113.64 & 0 & 0 & 0 & 0 & 1.54 \\ 0 & 0 & 0 & 9.86 & 0 & 0 & 0 & -9.86 \\ 0 & 0 & 0 & 0 & 331.71 & -294.12 & 0 & -37.59 \\ 0 & 0 & 0 & 0 & -294.12 & 294.12 & 0 & 0 \\ 0 & 0 & 0 & 0 & 0 & 0 & 76.92 & -76.92 \\ -19.46 & -37.71 & 0 & -9.86 & -37.59 & 0 & -76.92 & 523.78 \end{bmatrix}.$$

$$A = \begin{bmatrix} -0.0343 & 0 & 00.0338 & 0 & 0 & 0.0043 & 0 & \\ 0.0001 & -0.0124 & -0.0102 & 0.0001 & 0.0001 & 0.0001 & 0.0033 & 0.0001 \\ 0.0105 & -0.0141 & -0.0212 & 0.0205 & 0.0002 & 0.0002 & 0.0002 & 0.0002 \\ 0.0128 & 0 & 0 & -0.0761 & 0.0133 & 0.0141 & 0 & 0 \\ 0 & 0 & 0 & 0.0507 & -0.0133 & -0.0133 & 0 & 0 \\ 0 & 0 & 0 & 0.0338 & -0.0177 & -0.0200 & 0 & 0 \\ 0 & 0.0049 & 0.0049 & 0.0202 & 0.0053 & 0.0053 & -0.0104 & 0 \\ 0 & 0 & 0 & 0.0254 & 0.0066 & 0.0066 & 0.0032 & 0 \end{bmatrix},$$
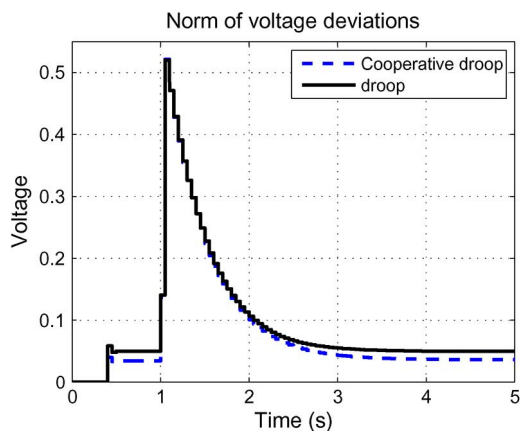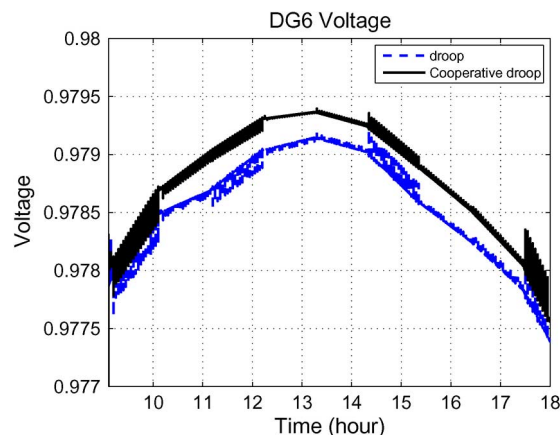
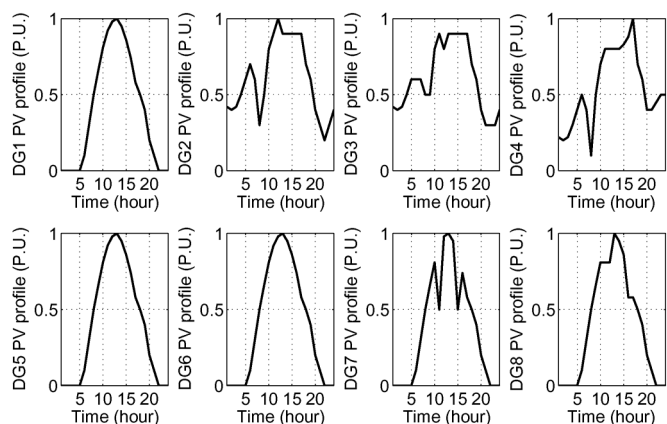Fig. 6.   Norm of voltage derivations from unity.

Fig. 7.   Profile of DGs.

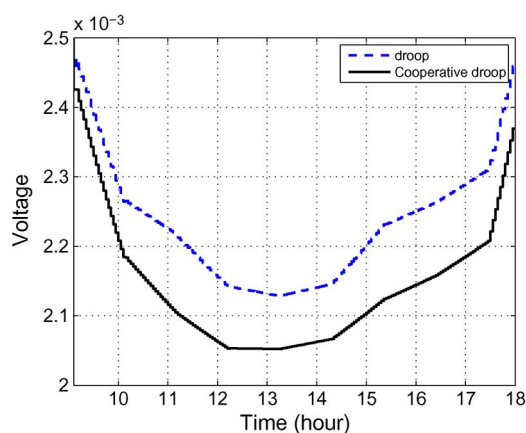
Fig. 8.   Voltage of DG3 in a daily operation.

Fig. 9.   Voltage of DG6 in a daily operation.

Fig. 10.   Norm of voltage deviations from unity in a daily operation.
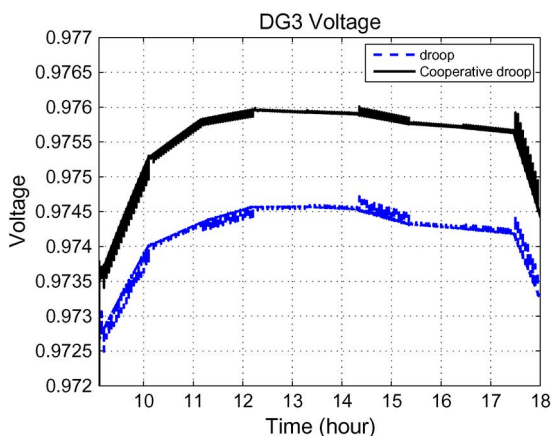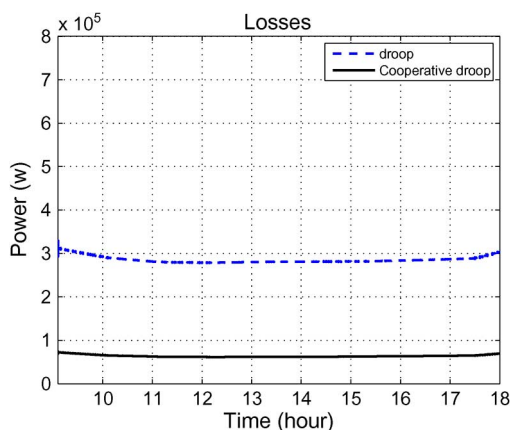

Fig. 11.   Norm of voltage deviations from unity in a daily operation.

As the second case study, a typical daily operation of the microgrid is simulated to evaluate its performance. The daily generation profiles of the DGs are provided in Fig. 7, and the simulation is for the time period from 9:00 am to 6:00 pm. Figs. 8 and 9 contain the voltages at DG3 and DG6, respectively; and Fig. 10 presents the norm of the voltage errors from unity at the DGs across the microgrid. Better voltage regulation is achieved by the proposed cooperative droop control. Fig. 11 shows the active power losses of the microgrid. It is noticed that the active power losses have been reduced by two thirds, or about 200 KW,

when compared with the conventional droop. This loss reduction amounts to 2% of the overall power rating of the microgrid under study, which is significant practically and theoretically.

Intuitively, cooperative droop control achieves better performance through locally sharing information among the neighboring nodes, and it approaches the optimal control if the information is shared across the microgrid. Simulation studies also show that the proposed control is robust with respect to the changes of both the physical grid and the (local) sensing/communication network(s).

VI. Conclusion

In this paper, advanced droop controls are designed, analyzed and compared for a DC microgrid with intermittent operation of DGs. First, an optimal control is designed for voltage/power regulation in the microgrid. The resulting control is nonlinear but can be approximated by a linear near-optimal control, and these controls require the full knowledge about the microgrid. It is shown that, if each DG operates by itself, the linear near-optimal control without any information about other nodes reduces to the conventional droop control as well as an adaptive control with a small leakage. Given that smart microgrids would have (intermittent) communication links to locally exchange information, a cooperative droop control is proposed to take advantage of the information distributively available. Stability and performance of the distributed cooperative droop control are analyzed to show that it includes the conventional droop control as a special case, provides the superior performance, and is robust with respect to the changes of distribution network and communication network.

APPENDIX A
PROOF OF THEOREM 1

Let $P_{g_i}^*$ and V_i^* be the (feasible) solution to the following algebraic equations:

$$\begin{cases} P_{g_i}^* - P_{l_i} = V_i^* \sum_{j \in \mathcal{V}_p} y_{ij} \left(V_i^* - V_j^* \right) & i \in \mathcal{V}_g \\ -P_{l_i} = V_i^* \sum_{j \in \mathcal{V}_p} y_{ij} \left(V_i^* - V_j^* \right) & i \notin \mathcal{V}_g. \end{cases} \quad (17)$$

It follows from (3) and (17) that, for $i \in \mathcal{V}_g$,

$$\begin{aligned} P_{g_i} &- P_{g_i}^* \\ &= V_i \sum_{j \in \mathcal{V}_p} y_{ij}(V_i - V_j) - V_i^* \sum_{j \notin \mathcal{V}_p} y_{ij} \left(V_i^* - V_j^* \right) \\ &= \sum_{j \in \mathcal{V}_p} y_{ij} \left[(V_i - V_i^*)(V_i - V_j) + V_i^*(V_i - V_j) - V_i^* \left(V_i^* - V_j^* \right) \right] \\ &= (V_i - V_i^*) \sum_{j \in \mathcal{V}_p} y_{ij}(V_i - V_j + V_i^*) + V_i^* \sum_{j \in \mathcal{V}_p} y_{ij} \left(V_j^* - V_j \right), \end{aligned} \quad (18)$$

and, for $i \notin \mathcal{V}_g$,

$$(V_i - V_i^*) \sum_{j \in \mathcal{V}_p} y_{ij} \left(V_i - V_j + V_i^* \right) + V_i^* \sum_{j \in \mathcal{V}_p} y_{ij} \left(V_j^* - V_j \right) = 0.$$

On the other hand, it follows from linear quadratic optimal control theory [23] that, under performance index (of sufficiently large T)

$$J_i = \beta_i \tau_i \left[P_{g_i}(T) - P_{g_i}^* \right]^2 + \int_{t_0}^{T} \left[k_i^2 \left(P_{g_i} - P_{g_i}^* \right)^2 + u_i^2 \right] dt,$$

the optimal steady-state tracker for system (2) is given by

$$u_i = -\frac{k_i^2}{1 + \sqrt{1 + k_i^2}} P_{g_i} + \frac{k_i^2}{\sqrt{1 + k_i^2}} P_{g_i}^* \quad (19)$$

$$= -\frac{k_i^2}{\sqrt{1 + k_i^2}} \left(P_{g_i} - P_{g_i}^* \right) + \frac{k_i^2}{1 + k_i^2 + \sqrt{1 + k_i^2}} P_{g_i}^*. \quad (20)$$

Substituting (18) into (20) yields control (5). Under control (19), system (2) becomes

$$\tau_i \dot{P}_{g_i} = -\sqrt{1 + k_i^2} P_{g_i} + \frac{k_i^2}{\sqrt{1 + k_i^2}} P_{g_i}^*,$$

which is exponentially stable with respect to the steady state

$$\lim_{t \to \infty} P_{g_i}(t) = \frac{k_i^2}{1 + k_i^2} P_{g_i}^*.$$

This completes the proof. □

APPENDIX B
PROOF OF LEMMA 1

It follows from (3) and (1) that, for constant-resistance loads, $P_G = \text{diag}\{V_i\} Y V$, where $\text{diag}\{V_i\}$ is the diagonal matrix consisting of V_i, $V = [V_1 \cdots V_n]^T$, and $P_G = [P_{G_1} \cdots P_{G_n}]^T$, where $P_{G_i} = P_{g_i}$ if $i \in \mathcal{V}_g$ and $P_{G_i} = 0$ if $i \notin \mathcal{V}_g$. It follows that, for any reasonable steady state P_G^* and V^*,

$$\begin{aligned} P_G - P_G^* &= \text{diag}\{V_i\} Y (V - V^*) + \text{diag}\{V_i - V_i^*\} Y V^* \\ &\approx \text{diag}\{V_i^*\} Y (V - V^*) + \text{diag}\{V_i - V_i^*\} Y V^* \\ &= H(V - V_*), \end{aligned} \quad (21)$$

where matrix H is defined by

$$H = [H_{ij}] \in \Re^{n \times n}, \quad H_{ij} = \begin{cases} y_i + Y_{ii} & \text{if } i = j \\ Y_{ij} & \text{if } i \neq j. \end{cases} \quad (22)$$

It follows from [18] that H is a symmetric, nonsingular M-matrix.

Let T be the permutation matrix such that $TP_G = [P_g \ 0]^T$, where $P_g = \text{vec}\{P_{g_i}\}$ for $i \in \mathcal{V}_g$. It follows that $TV = [V_g \cdots]^T$, where $V_g = \text{vec}\{V_i\}$ for $i \in \mathcal{V}_g$. Applying matrix T to (21) and then partitioning the resulting matrix yield

$$\begin{aligned} \begin{bmatrix} P_g - P_g^* \\ 0 \end{bmatrix} &= THT^T \begin{bmatrix} V_g - V_g^* \\ \vdots \end{bmatrix} \\ &\triangleq \begin{bmatrix} E_{gg} & E_{g0} \\ E_{g0}^T & E_{00} \end{bmatrix} \begin{bmatrix} V_g - G_g^* \\ \vdots \end{bmatrix}. \end{aligned}$$

Solving the above equation renders relationship (15) between P_g and V_g, where $H_{gg} \triangleq E_{gg} - E_{g0}^T E_{00}^{-1} E_{g0}$. Again, it can be shown that reduced-order matrix H_{gg} is a symmetric, nonsingular M-matrix. Hence, its inverse is a positive matrix, and relative values of off-diagonal entries are monotonely increasing functions of the distances among the DGs. □

APPENDIX C
PROOF OF THEOREM 2

It follows from system (2) and cooperative droop control (12) that, among all possible steady-state solutions P_g^* and V_g^*,

$$\text{diag}\{\tau_i\} \dot{P}_g = -\text{diag}\{\varepsilon_i\} \left(P_g - P_g^* \right) + D \left(V_g - V_g^* \right) + \delta, \quad (23)$$

where $\mathbf{1}$ is the vector of 1s, and $\delta = -\text{diag}\{\varepsilon_i\} P_g^* + D(V_g^* - \mathbf{1})$. Hence, the specific steady state achieved under cooperative droop control (12) satisfies the relationship of $\delta = 0$, that is,

$$\text{diag}\{\varepsilon_i\} \left(P_g - P_g^* \right) = D \left(V_g^* - \mathbf{1} \right) = D V_g^*, \quad (24)$$

where the last equation comes from the fact that D has zero row sums.

For the steady state satisfying (24), one can substituting (15) into (23) and obtain

$$\text{diag}\{\tau_i\} \dot{P}_g = \left[-\text{diag}\{\varepsilon_i\} + D H_{gg}^{-1} \right] \left(P_g - P_g^* \right).$$

Asymptotic stability and local exponential convergence can be concluded using Lyapunov function matrix M.

Recall that cooperative droop control (12) includes the two extreme cases: conventional droop control (10) if S is the identity matrix and, if $S = \mathbf{1}\mathbf{1}^T$, near-optimal control (9) corresponding to $V_i^* = 1$ for $i \in \mathcal{V}_g$. It follows from theorem 1 and from the discussions of (7), (8) and (9) that, as cooperative droop control (12) has more information, it becomes closer to near-optimal control (9) and hence the node voltages become closer to 1. $\qquad\square$

REFERENCES

[1] M. E. Baran and N. R. Mahajan, "DC distribution for industrial systems: Opportunities and challenges," *IEEE Trans. Ind. Appl.*, vol. 39, no. 6, pp. 1596–1601, Nov. 2003.

[2] A. Maknouninejad, W. Lin, H. G. Harno, Z. Qu, and M. A. Simaan, "Cooperative control for self-organizing microgrids and game strategies for optimal dispatch of distributed renewable generations," *Energy Syst.*, vol. 3, no. 1, pp. 23–60, 2012.

[3] H. Ikebe, "Power systems for telecommunications in the IT age," in *Proc. IEEE INTELEC*, Yokohama, Japan, Oct. 2003.

[4] A. Kwasinski and C. N. Onwuchekwa, "Quantitative evaluation of dc microgrids availability: Effects of system architecture and converter topology design choices," *IEEE Trans. Power Electron.*, no. 3, pp. 835–851, Mar. 2011.

[5] D. Nilsson and A. Sannino, "Efficiency analysis of low- and medium-voltage dc distribution systems," in *Proc. IEEE PES Gen. Meet.*, Washington, DC, USA, Jun. 2004, vol. 2, pp. 2315–2321.

[6] G. S. Seo, J. Baek, K. Choi, H. Bae, and B. Cho, "Modeling and analysis of dc distribution systems," in *Proc. 8th Int. Conf. Power Electron.—ECCE Asia*, The Shilla Jeju, Korea, May 2011, vol. 2, pp. 223–227.

[7] E. W. Kimbark, "DC transmission," *Direct Current Transm.*, vol. 1, no. 6, pp. 148–152, Nov. 1971.

[8] H. Kakigano, Y. Miura, T. Ise, and R. Uchida, "Dc micro-grid for super high quality distribution-system configuration and control of distributed generations and energy storage devices," in *Proc. IEEE Power Electron. Specialists Conf.*, Washington, DC, USA, Jun. 2006, pp. 1–7.

[9] G. Byeon, T. Yoon, S. Oh, and G. Jang, "Energy management strategy of the dc distribution system in buildings using the ev service model," *IEEE Trans. Power Electron.*, vol. 28, no. 4, pp. 1544–1554, Apr. 2013.

[10] F. Katiraei and M. Iravani, "Power management strategies for a microgrid with multiple distributed generation units," *IEEE Trans. Power Syst.*, vol. 21, no. 4, pp. 1821–1831, Nov. 2006.

[11] F. Katiraei, R. Iravani, N. Hatziargyriou, and A. Dimeas, "Microgrids management," *IEEE Power Energy Mag.*, vol. 6, no. 3, pp. 54–65, 2008.

[12] F. Katiraei, M. Iravani, and P. Lehn, "Small-signal dynamics model of a micro-grid including conventional and electronically interfaced distributed resources," *IET Gener., Transm., Distrib.*, vol. 1, no. 3, pp. 369–378, May 2007.

[13] M. Prodanovic and T. Green, "High-quality power generation through distributed control of a power park microgrid," *IEEE Trans. Power Del.*, vol. 53, no. 5, pp. 1471–1482, Oct. 2006.

[14] Y. Abdel-Rady, I. Mohamed, and E. F. El-Saadany, "Adaptive decentralized droop controller to preserve power sharing stability of paralleled inverters in distributed generation microgrids," *IEEE Trans. Power Electron.*, vol. 23, no. 6, pp. 2806–2816, Nov. 2008.

[15] J. C. Vasquez, J. M. Guerrero, A. Luna, P. Rodriguez, and R. Teodorescu, "Adaptive droop control applied to voltage-source inverters operating in grid-connected and islanded modes," *IEEE Trans. Ind. Electron.*, vol. 56, no. 10, pp. 4088–4096, Oct. 2009.

[16] H. Alatrash, A. Mensah, E. Mark, G. Haddad, and J. Enslin, "Generator emulation controls for photovoltaic inverters," *IEEE Trans. Smart Grid*, vol. 3, no. 2, pp. 996–1011, Jun. 2012.

[17] J. M. Guerrero, J. C. Vasquez, J. Matas, L. G. de Vicuna, and M. Castilla, "Hierarchical control of droop-controlled ac and dc microgrids—A general approach toward standardization," *IEEE Trans. Ind. Electron.*, vol. 58, no. 1, pp. 158–172, Jan. 2011.

[18] Z. Qu, *Cooperative Control of Dynamical Systems*. London, U.K.: Springer, 2009.

[19] H. Xin, Z. Qu, J. Seuss, and A. Maknouninejad, "A self-organizing strategy for power flow control of photovoltaic generators in a distribution network," *IEEE Trans. Power Syst.*, vol. 26, no. 3, pp. 1462–1473, 2011.

[20] A. Maknouninejad, Z. Qu, J. Enslin, and N. Kutkut, "Clustering and cooperative control of distributed generators for maintaining microgrid unified voltage profile and complex power control," in *IEEE PES Transm. Distrib. Conf.*, Orlando, FL, USA, May 2012, pp. 1–8.

[21] K. S. Narendra and A. M. Annaswamy, *Stable Adaptive Systems*. Englewood Cliffs, NJ, USA: Prentice-Hall, 1989.

[22] Z. Qu, *Robust Control of Nonlinear Uncertain Systems*. New York: Wiley, 1998.

[23] F. L. Lewis, *Optimal Control*. New York: Wiley, 1986.

Ali Maknouninejad (S'08–M'13) received his electrical engineering B.Sc from University of Tehran, Tehran, Iran, in 2001. Then, he joined Power Supply Production (PSP) Co., Tehran, as a Research Engineer and worked on the design and construction of DC/AC inverter converters up to 30 KVA for use in UPS systems. He attended University of Central Florida (UCF), Orlando, FL, USA, in 2008, received his M.Sc. in Electrical Engineering in 2010, and then completed his Ph.D. study in May 2013. His research interests include smart grid and distributed generator control and stability analysis.

Zhihua Qu (M'90–SM'93–F'09) received the Ph.D. degree in electrical engineering from the Georgia Institute of Technology, Atlanta, GA, USA, in June 1990. Since then, he has been with the University of Central Florida (UCF), Orlando, FL, USA. Currently, he is the SAIC Endowed Professor in College of Engineering and Computer Science, Professor and Chair of Electrical and Computer Engineering, and the Director of FEEDER Center (one of DoE-funded national centers on distributed technologies and smart grid). His areas of expertise are nonlinear systems and control, with applications to energy and power systems. In energy systems, his research covers such subjects as low-speed power generation, dynamic stability of distributed power systems, anti-islanding control and protection, distributed generation and load sharing control, distributed VAR compensation, distributed optimization, and cooperative control. Dr. Qu is currently serving as an Associate Editor for *Automatica* and *IEEE Access*.

Frank L. Lewis (S'78–M'81–SM'86–F'94) received the B.S. degree in physics/electrical engineering and the M.S.E.E. degree from Rice University, Houston, TX, USA, the M.S. degree in aeronautical engineering from the University of West Florida, Pensacola, FL, USA, and the Ph.D. degree from the Georgia Institute of Technology, Atlanta, GA, USA. He is a Distinguished Scholar Professor and Moncrief-O'Donnell Chair with the Automation and Robotics Research Institute (ARRI), University of Texas at Arlington (UTA), TX, USA. He works in feedback control, intelligent systems, distributed control systems, and sensor networks. Dr. Lewis is also a Fellow of the International Federation of Automatic Control (IFAC) and a Fellow of the U.K. Institute of Measurement and Control. He is a Professional Engineer in the state of Texas and a Chartered Engineer in the U.K.

Ali Davoudi (S'04–M'11) received his Ph.D. in Electrical and Computer Engineering from the University of Illinois, Urbana-Champaign, USA, in 2010. He received B.Sc. and M.Sc. degrees in Electrical and Computer Engineering from Sharif University of Technology, Tehran, Iran, and The University of British Columbia, Vancouver, Canada, in 2003 and 2005, respectively. He is currently an Assistant Professor at the Electrical Engineering Department, University of Texas, Arlington, TX, USA. He worked for Solar Bridge Technologies, Texas Instruments Inc., and Royal Philips Electronics. He is an Associate Editor for IEEE TRANSACTIONS ON INDUSTRY APPLICATIONS. His research interests are various aspects of modeling, simulation, and control of power electronics, energy conversion systems, and finite-inertia power systems.